Semi-Emperical Model to Determine Liquid Velocity and Pressure Loss of Two-Phase Flow in A Horizontal Bend–Part I (Stratified Flow)

Amir Alwazzan*

OneSubsea (a Cameron-Schlumberger Company) 4646 W. Sam Houston Parkway – North, Houston, TX 77041, USA

Abstract: The objectives of this study are to conduct a thorough literature review on the subject of multiphase flow through bends and to develop and evaluate a semi-empirical model to determine liquid velocity and pressure loss during stratified gas-liquid flow in a horizontal bend. The model is based on incorporating the momentum balance equations of both phases (air and water). Extensive experiments were carried out to acquire data using air and water in a 0.05 m diameter horizontal pipe simulator with an intermediate bend of 0.5 m radius of curvature.

The results show that due to the disturbance nature of the two-phase flow in general, it is quite convenient to describe the pressure drop in terms of the energy loss. It was also found that stratified flow does not cause a significant change in the energy during the flow along the bend traverse due to its stable nature. The semi-empirical model developed for predicting the superficial water velocity during stratified flow shows an acceptable agreement with the experimental data.

The work presented in this paper may help flow assurance, production, pipeline and process engineers to have reliable design and operations through counting for the losses caused by such components.

Keywords: Two-phase, bends, stratified flow, pressure loss.

1. INTRODUCTION

Structural integrity of pipelines and piping systems and its impact on the fluids behaviors are of paramount importance for flow assurance, production and process engineers. Good understanding of this subject could provide a great value to oil and gas projects and have an impact on both CAPEX and OPEX.

Bends are frequently found in offshore and onshore oil and gas production systems. These structures could pose abrupt changes to the flow parameters (manily pressure and velocities) leading to potential issues with the conduit integrity.

The head losses, which occur in fully developed flowlines, can be calculated by using conventional friction factor charts even though our knowledge of turbulence is incomplete. For many pipeline installations, the 'minor' head losses in the fittings, *e.g.* bends, valves, expansion and contractions, can outweigh the 'major' straight pipe losses.

Prediction of head losses and liquid velocities in single-phase flows has been well covered in the literature and industry. However, there is still a lack of adequate studies to better understand the impact of such fittings during multiphase flows.

*Address correspondence to this author at the OneSubsea (a Cameron-Schlumberger Company) 4646 W. Sam Houston Parkway – North, Houston, TX 77041, USA; Tel: +1 713 8855275;
E-mail: Amir.Alwazzan@OneSubsea.com

While the complexity of multiphase flow is mainly due to the nature of its turbulence nature associated with different flow patterns and abrupt transitioning between them, the majority of the works done on multiphase flow through bends have not really considered the flow patterns as a controlling factor. In other words, very little works have differentiated between the different flow regimes of multiphase flow while passing a fitting like a bend.

This work represents the first phase of a project to thoroughly investigate the effect of different flow patterns on the pressure drop and liquid velocity changes while passing a horizontal bend.

2. THEORY

2.1. Single-Phase Flow

An important aspect of the design of a fluid flow system is the evaluation of the pressure loss in fluid dynamics subcritical single-phase as well as two-phase flow.

Theoretical and numerical studies for investigating the stationary entry of single-phase fluid flow in a bend have been performed [1-7].

Experimental analyses were made [8-15]. Most of these investigations dealt with uniform entry flow where immediately after the entry into the bend, a secondary flow is set up. This flow is dominated by the build-up of an axial boundary layer.

E-ISSN: 2409-787X/15

Investigators have established the effect of the secondary flows on bend flow characteristics through measurement of velocity field, Reynold's stresses and bend loss coefficient at various radius ratios [16].

When the fluid flows through abend, the curvature causes a centrifugal force directed from the momentaneous center of curvature to the outer wall. This force and the presence of a boundary layer at the wall along with the fluid adhesion to the wall generate secondary flow ideally organized in two identical eddies, as shown in Figure **1**:

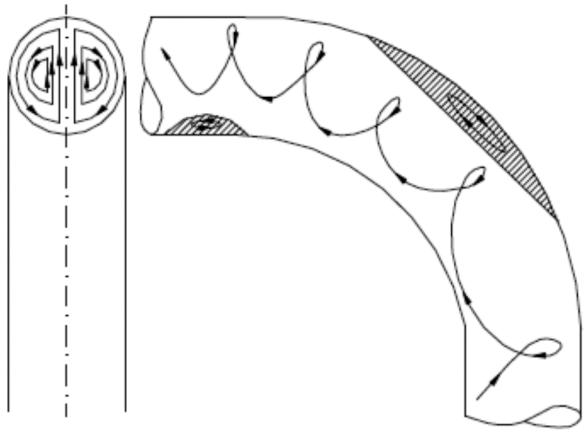

Figure 1: Streamlines of the secondary flow, respired vortex pair, in the longitudinal section and the cross section of a 90^{o} bend for the case of a symmetrical inlet stagnation pressure distribution [17].

Basically, the fluid in the core moves outwards and in the region near the wall inwards. The secondary flow is superimposed to the main stream along to the tube axis, imposing a helical shape to the stream lines. This effect of the bend on the structure of the flow was carefully reviewed and discussed [18-20].

Azzi *et al.* [21] stated that the total bend pressure loss in adiabatic flow is caused by convention and assumed to consist of contributions due to wall friction and momentum exchange between the phases, vortex detachment, secondary flow generation and the additional loss in downstream tangent to recover the initial symmetric velocity profile. In principle, these contributions can be summarized under friction and form losses.

The method generally used for the determination of the pressure loss is best explained on the basis of a graphical procedure, as shown in Figure **2**:

The course of the mean static pressure along the piping during stationary flow, sufficiently far away upstream and downstream of the bend, is extrapolated onwards and backwards to the inlet and outlet of the bend. The extrapolated difference in static pressure gives the bend pressure loss (ΔPb). It is obvious that this loss still includes the additional friction of the onset flow in the two and six inner pipe diameters.

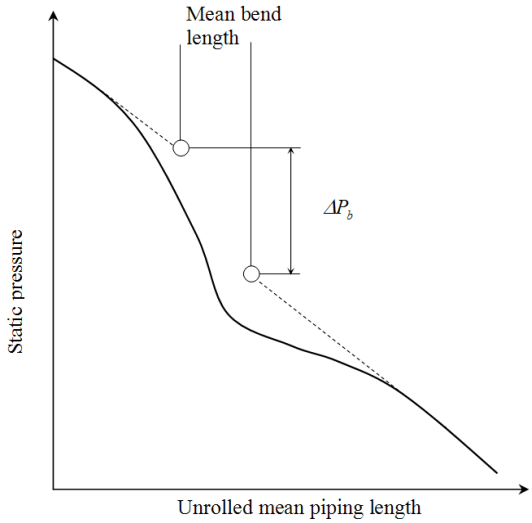

Figure 2: Mean static pressure along a horizontal pipe of constant diameter with an interjacent bend during incompressible flow and definition of the bend pressure loss [21].

In fact, these contributions are usually considered negligibly small in comparison with the total pressure loss. As such, the total pressure loss developed in this way can be as severe as a local quantity in a one dimensional based fluid dynamic design of piping systems.

From this description of the pressure loss derivation it becomes also clear that the simple application of this procedure is restricted to the cases of incompressible and subcritical compressible pipe flows, where the density and/or mass flow quality change along the bend is negligibly small.

In general, the flow characteristics in a bend for a single-phase fluid are reasonably well understood.

2.2. Two-Phase Flow

In two-phase flow, the bend pressure loss is additionally increased due to the dissipation caused by the separation and remixing of the gas and the liquid phase. In addition, the gravitational force influences the flow behavior and flow pattern changes in horizontal flow.

In general, studies in bends for a two-phase fluid flow are relatively few in number. Several models are

devoted to the single-phase flow bend pressure loss prediction [12,17,22,23].

Concerning the two-phase flow, which can exhibit a wide range of phase configurations as a consequence of the deformable interphase; few systematic investigations of the bend pressure loss were performed over the last decades.

An overview regarding the effect of the elbow on the structure of the two-phase flow was put forward [24-26]. However, in both flow types, this secondary flow along with local vortex generation and wall detachment causes an excess pressure loss compared to that in a straight pipe with the same mean length and diameter.

Recently, good studies have been carried out using the CFD (Computational Fluid Dynamics) by Khaksafard *et al*. [27] and STAR-OLGA coupling by Xing and Yeung [28] to investigate slug flow impact on the pipe bends. Belfroid et al. [29] measured the forces exerted on a one diameter horizontal bend and T-junctions due to multiphase flow. They concluded that the measured amplitude was between 1 and 10 times the liquid momentum based on the mixture velocity.

In general, the respective bend pressure loss in two-phase flow is by convention related to that in single-phase flow. Hence, the usual way of predicting this indispensable quantity is addressed first for the sake of completeness [21]. It is characterized in one-dimensional single-phase flow by dimensionless loss coefficient, *K* where:

$$K = \Delta P_b / \rho V^2/2 \quad (1)$$

where ρ is the fluid density and *V* is the mean inlet flow velocity.

This coefficient stands for the number of velocity heads required to account for the bend loss. With this relationship, it slips into the role of a physical quantity being primarily a function of the parameters governing the flow turbulence intensity, the inlet velocity profile as well as the tendency to induce a secondary flow.

These parameters are partly included in the Reynolds number or in the Dean number incorporating the Reynolds number and the relative bend curvature and representing the ratio of the geometric average of the inertial and centrifugal forces to the viscous force. It serves in special cases for reducing the number of variables. The relative mean wall roughness and the geometric parameters as the angle of the bend and the relative bend curvature could be other main parameters, as shown in Figure **3**:

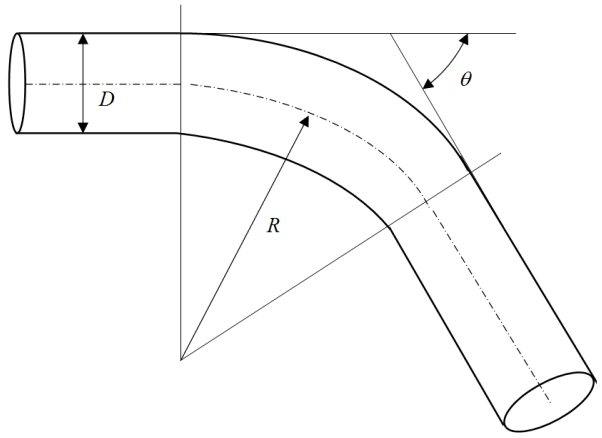

Figure 3: Geometric parameters of a bend.

The roundness of the flow cross section on the other hand is assumed as given. A simple method only valid just for the assessment of the magnitude of the two-phase flow bend pressure loss is to introduce the homogeneous flow density $(1/\rho_{homogeneous} = x^*/\rho_{gas} + (1 - x^*)/\rho_{liquid})$ in equation (1) instead of the fluid density of each phase in particular.

It is important to highlight that the works presented above did not specify the flow pattern for which the correlations were developed.

A research has been conducted to study the pressure drop in two-phase solid-fluid flows through bends. These results have been reviewed and presented by Alwazzan [30].

2.3. Parameters of the Pressure Loss of the Two-Phase Flow Through Bends

In accordance with the independent parameters valid in stationary single-phase flow, the two-phase flow pressure loss is considered to be dependent on the flow rates of both phases, the macroscopic phase state and transport properties (*i.e.* density and viscosity of each phase), the geometric parameters of the bend and on the local gravity where the bend plane is not positioned horizontally or if the flow occurs under micro gravity condition.

The established flow pattern is a result of interaction of these primary parameters, hence it is not considered as an independent Figure. Furthermore, the mean pipe wall roughness can be excluded as a parameter since it generally has a minor influence on two-phase flow compared to that on single-phase flow. Additionally, the

surface tension is also ignored as its force is generally small compared to the inertial and pressure force in flow systems under a pressure sufficiently above that of the atmosphere.

The physical relationship between the primary parameters and the pressure loss is attempted to explain qualitatively based on the basis of a thinkable variation of an independent single parameter while keeping the others constant. For reducing the number of Figures, the flow rate of each phase is as usual in two-phase flow substituted by the total mass flow rate and the mass flow quality. Though it is not measurable, it becomes a dominant primary parameter while the former strong effect of the mass flow rates is drastically reduced.

Additionally, the densities and viscosities of both phases are included in a density and viscosity ratio. In fact, the gas-phase dynamic viscosity remains always in the same order of magnitude under the usual technical conditions far beyond the thermodynamic critical pressure so that its effect is considered small when compared to that of the liquid viscosity. Basically, it acts then only as a means for non-dimensionalization. Finally, a usual procedure is to normalize the curvature radius with the bend pipe diameter.

The merged variables to be considered in the analysis of the interaction would be total mass flow rate, mass flow quality, density and viscosity ratios and dimensionless curvature and gravity constant.

The qualitative interrelationship between the merged variables, design parameters and the bend pressure loss is as follows: pressure drop will increase with larger total mass flow rate as then the velocity of each phase is higher. This basic behavior is expected similarly to the single-phase flow theory. The same tendency would be valid if the quality is only enlarged as then again higher velocities prevail due to the larger volumetric gas or vapor flow rate and the only marginally reduced liquid mass flow rate. This is solely valid for the case that the densities differ substantially.

On reducing the density ratio, *e.g.*, by increasing the system pressure, the pressure loss will decrease as in the case of a constant mass flow rate and quality then the gas/vapor volume and, thus, the mean velocities are lower.

A change of the viscosity ratio, practically only achievable by a higher or lower liquid phase viscosity in a two-component mixture, induces corresponding changes to the wall shear stress while the momentum exchange between the phases would change in opposite directions. As this latter mechanism is affected to a lesser extent (in total for otherwise equal flow conditions) larger or smaller pressure loss will be consequence. Finally, an increase of the curvature radius while retaining ideally a fixed mean bend length would decrease the intensity of the induced secondary flow and, therefore, lead in relation to a lower pressure loss.

Ultimately, for an identified curvature radius the lower limit should be equal to the pressure loss of a straight pipe. The gravity influences the pressure loss in non-horizontal flow due to the difference in shear stress distribution. However, this effect is only marginal. By far more stringent in its effect is that the gravitational force will interact with the centrifugal force causing complex phenomena such as phase inversion, flooding and flow reversal, which expectedly lead to a higher pressure loss than when the bend is positioned horizontally. The gravity constant can serve also as a scaling factor for obtaining local quantities when the bend flow occurs under micro or macro gravity conditions.

Independent parameters with relatively minor or secondary influence on the pressure loss are expected to be besides of the already discarded mean (natural) wall roughness and roundness of the cross section as well as surface tension. These parameters like the physi-chemical properties, wall wetting and coalescence behavior or mechanical disproportioning of the gas phase as well as the state change of the unheated mixture are considered as adiabatic here.

With this physical understanding, the independent primary parameters should be found in the pressure loss correlations as equation variables. The extent to which this is actually realized will be considered sub-sequently.

3. MODELING OF THE PRESSURE DROP OF THE STRATIFIED FLOW

Considering a steady-state air-water stratified flow in a horizontal bend, a momentum balance on each phase yields:

$$\frac{\partial}{\partial t}\left(\rho_L A_L U_L\right)+\frac{\partial}{R\partial\theta}\left(\rho_L A_L U_L^2\right)= \tau_L S_L+\tau_i S_i-A_L\frac{\partial P_{iL}}{R\partial\theta}-\rho_L A_L g\cos\gamma\frac{\partial h_L}{R\partial\theta} \quad (2)$$

$$\frac{\partial}{\partial t}\left(\rho_G A_G U_G\right)+\frac{\partial}{R\partial\theta}\left(\rho_G A_G U_G^2\right)= \\ -\tau_G S_G-\tau_i S_i-A_G\frac{\partial P_{iG}}{R\partial\theta}-\rho_G A_G g\cos\gamma\frac{\partial h_L}{R\partial\theta} \quad (3)$$

The experimental data such as the superficial air and water velocities and the water film height could be used to find pressure drop under force balance for steady and fully developed flow in bend. For the steady-state flow, assuming that the pressure drop is the same for both phases, liquid height gradient $\frac{\partial h_L}{R\partial\theta}$ could be adjusted for pressure drop gradient equality in both air and water phases. Recalling that $\frac{\partial h_L}{R\partial\theta}$ has to have a value since the water film height varies significantly across the bend. Hence, the positive values of h_L reflect that the liquid film increases while the negative values indicate that the liquid film decreases. It is necessary to highlight that for the same air and water velocities, the comparisons were done between the air and water pressure drops at each of the inlet and outlet stations.

4. EXPERIMENTAL FACILITY

Extensive experiments were performed in an indoor low-pressure two-phase flow loop. A schematic diagram of the experimental facility is shown in Figure **4** below:

Air and water are mixed in a mixing chamber at the inlet of a transparent polycarbonate pipe of 0.05 m diameter to form an air-water two-phase flow mixture. The air-water mixture then flows through a Plexiglas flow line consists of horizontal straight section of a 4.5 m long, 0.5 m radius of curvature long bend and 3.5 m long horizontal straight section before discharging into the water storage tank.

Air is supplied from the receiver of a two-stage compressor. The air flow rate is measured using an orifice meter with a 1.54 cm diameter orifice plate designed according to the American Gas Association standard. The flow rate was calibrated using a DWYER gas tube flow meter, which is able to measure up to 400 SCFM.

Water is drawn from the storage tank by a CMG CP25 DRESSER mono pump. To minimize the pulsation associated with off-design pumping operation when the required flow is small, a bypass is used to divert the excess water flow back to the storage tank. A heating system is installed in the water tank to control the water temperature at 27 ^{o}C. Water flow rate is measured by a digital flow sensor which converts the flow to an electric pulse signal for readout by a digital flow meter.

To collect empirical data, precision sensors (*Lucas Schaevitz PS 3363-0005-030PV*) have been mounted flush to the bottom of the inlet and outlet parts of the bend to get the water pressure. The air pressure was acquired by mounting sensors to the upper part of the

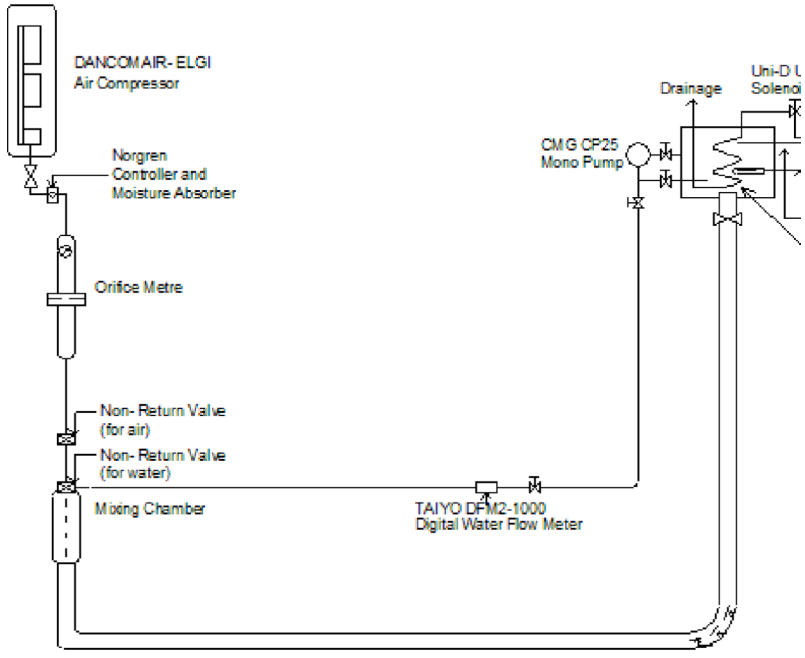

Figure 4: Schematic diagram of the experimental facility.

bend's inlet and outlet and four other locations distributed uniformly along the bend section.

By means of an Automatic Data Acquisition System (ADAS) composed by a high speed PC and a Data Acquisition Card (*Keithly – DAS 802 A/D*), the pressure signals were detected for 120 seconds with a capturing rate of 20 Hz and processed by the Test Point 3.30 software, which was able to remove the noise associated with the signals by filtering the readings. The data then was sent to Excel for further processing. Both signals were cross correlated to obtain its characteristic delay time, then, this value was correlated with the distance between the two sensors to get the characteristic velocity of the group of slugs detected. During the runs associated with slug flow, sensors were also connected at the top in order to measure the air pressure simultaneously.

The pressure sensors have a pressure range of 0-30 psig and an offset of ± 0.25%. The two pressure sensors has been calibrated by comparing the readings they give for the hydrostatic pressure generated by a static water level in the pipe with the pressure values calculated using the measured wetted perimeter. A 50 Hz rate of capturing was used for 10 seconds duration for each water height. The results are depicted in Figure **5**.

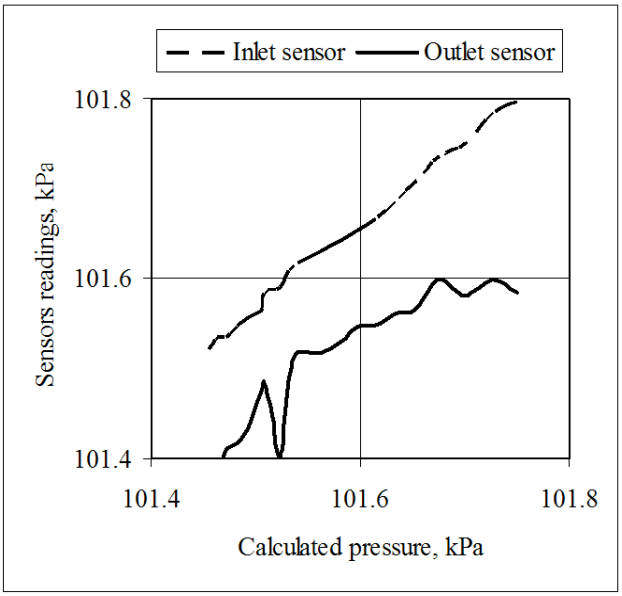

Figure 5: Calibration of the pressure sensors.

Visual observations have been made on the flow pattern variations at the inlet and along the long bend during the experiment. A fixed high-speed and high resolution camera was used to capture images for the two-phase flow through the loop. The video imaging system comprised of a JVC Color CCTV camera model TK-C1380, a JVC View Finder model TM-A14PN-S, a JVC Video Recorder model SR-L910E, a Pinnacle Frame Grabber model DV500 A/D with a software package of Adobe Premier version 5.1 running on a Pentium III computer. In addition to the high-speed camera recordings, each test was recorded with a hand camera. The recordings were used later to confirm visual observations. The flow is then broadly classified as stratified smooth, stratified wavy or slugged.

Wetted perimeter has been directly measured at several locations along the test bend pipe and from which the liquid film thickness was calculated. The varying parameters were the two phases velocities with the ranges of 2.22-8.97 m/sec for air and 0.0094-0.0778 m/s for water.

5. RESULTS AND DISCUSSION

In order to assess the pressure drop correlations exist in literatures against the experimental data acquired from this work, the pressure time series were averaged for all the flow patterns generated during the flow. However, a remarkable gap was found between the experimental pressure drop values and the calculated ones using the correlations of [31-35]. This is due to the fact that the formulation of these correlations is based on considering the flow as a homogeneous one as it is clear in calculating the different parameters while the experiments have been conducted for stratified, intermittent and slug flows. It is also important to remember that the vast difference between the nature of each of these flow patterns affect the role and contribution of each of the pressure drop parameters.

It seems that due to the pulsation associated with the pressure drop readings, especially the severe ones associated with the slug flow runs, endless possibilities could rise for interpreting the information acquired. For example, the inlet pulse is high while the outlet pulse is low and vice versa, the inlet pressure is rising while the outlet is dropping, etc. Averaging overtime tends to underestimates the actual pressure drop which the pump/compressor have got to overcome. In order to overcome such discrepancies, the use of the power spectrum, which accounts for the summation of energy of all the harmonic components, is a good indication of energy loss.

5.1. Pressure Drop of Stratified Air-Water Flow Across a Horizontal Bend

Along with the raw signals, the Cross-Correlation Function (CCF) has been implemented to analyze the time series results. In signal processing, CCF is a measure of similarity of two waveforms as a function of a time-lag applied to one of them. It is commonly used to search a long duration signal for a shorter known feature.

The time series of both air and water pressure readings during stratified flow were well recognized with their smooth and small amplitude fluctuations. In other words, no recognizable peaks were noticed in the sensors readings during the stratified flow.

Typical example of the waveform time series of the water phase acquired during the flow of stratified flow pattern is shown in Figure **6**.

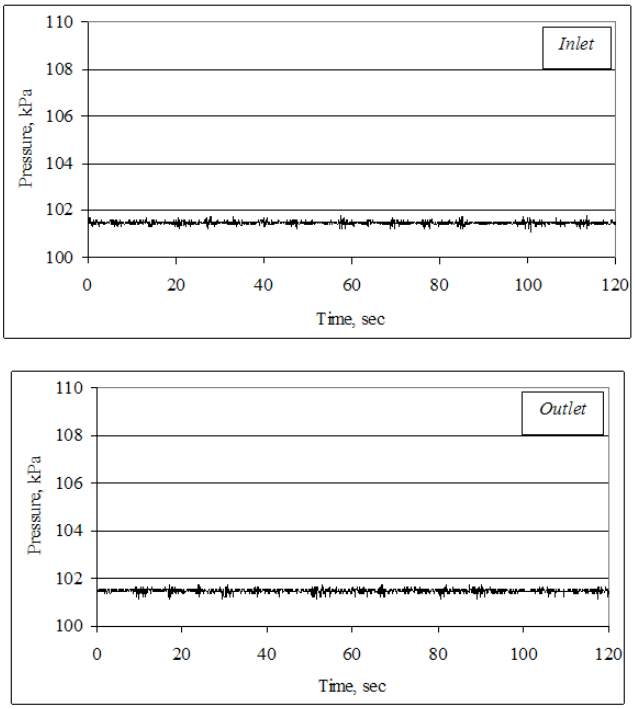

Figure 6: Typical pressure trace for stratified flow with U_{LS} of 0.0094 and and U_{LG} of 2.22 m/sec.

The features of the two waveforms shown in Figure **6** are almost identical and the principal characteristic is that the wave variation is small and the frequencies of the waves are roughly similar. This implies that the pressure value at the inlet and outlet of the bend is the same and no significant pressure drop exists. The averaged values of the pressure readings for the inlet and outlet points are 101.47 and 101.46 kPa, respectively. This is consistent with the physics and nature of the stratified smooth flow. Hence, the pressure signals are sensed almost instantaneously from the upstream to the down stream points since flow conditions at the bend inlet and outlet are almost identical to each other. This leads to the conclusion that during this flow, the two signals were sensing the same hydrostatic pressure generated by the water film height, which is almost the same at the inlet and the outlet of the bend. This is also borne out by the CCF, which gives a lag time of almost zero, as depicted in Figure **7**.

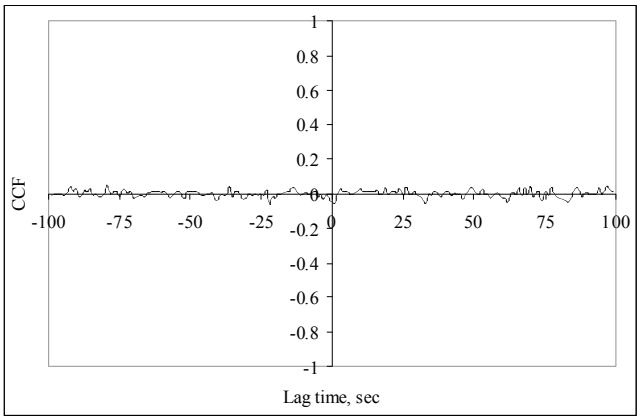

Figure 7: The CCF of the inlet and outlet time series for U_{LS} of 0.0094 and U_{LG} of 2.22 m/sec.

The lag time of a signal is the time corresponds to the maximum CCF value. It is obvious that Figure **7** does not show any recognizable CCF value.

Increasing the gas velocity to generate stratified wavy flow has a direct impact on the CCF results as shown in Figure **8** below:

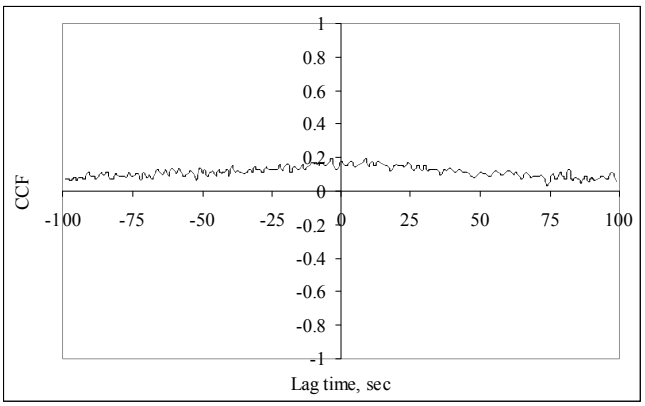

Figure 8: The CCF of the inlet and outlet time series for U_{LS} of 0.0094 and U_{LG} of 7.72 m/sec.

Figure **8** shows that with high gas velocity, the CCF gains values but there is no particular peak corres-

ponds to the lag time. The interpretation is that the two time series are somehow correlated to each other and tend to form a peak but yet to have a clear and sharp one. This is mainly due to the fact that during these particular runs, the interfacial waves posses higher velocities during traveling downstream the bend.

The power spectrum density, sometimes called the mean squared spectral density, relates the energy distribution of the pressure fluctuation to the frequency domain.

The power spectra density for the time series shown in Figure **6** is shown in Figure **9** below:

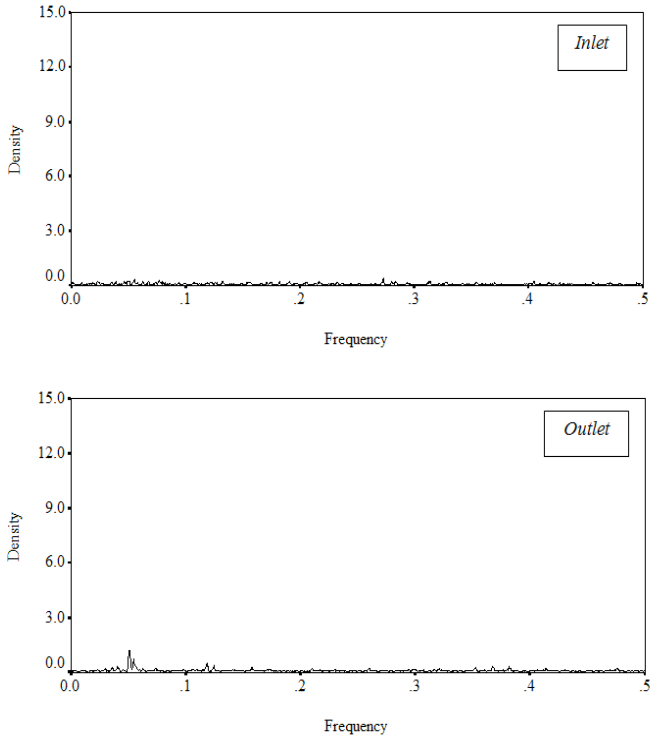

Figure 9: The Power Spectral Density for U_{LS} of 0.0094 and U_{LG} 2.22 m/sec.

At both the inlet and outlet of the bend points, the frequency of the energy fluctuations was distributed over a wide domain frequency. While there is no energy fluctuation appears along the domain axis of the inlet point, there is a tiny increment appears in the beginning of the dominant frequency at the outlet measurement point. This reflects a small value of disturbance at this point and it could explain the role of the bend in generating the disturbance.

The results of the power spectra analyses of other runs with stratified wavy flow are depicted in Figures **10** and **11**:

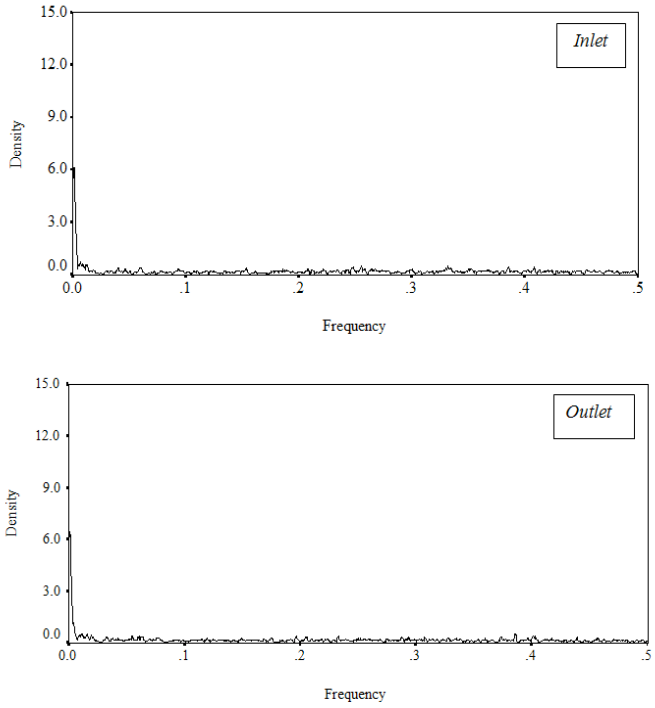

Figure 10: The Power Spectral Density for U_{LS} of 0.0094 and U_{LG} of 7.72 m/sec.

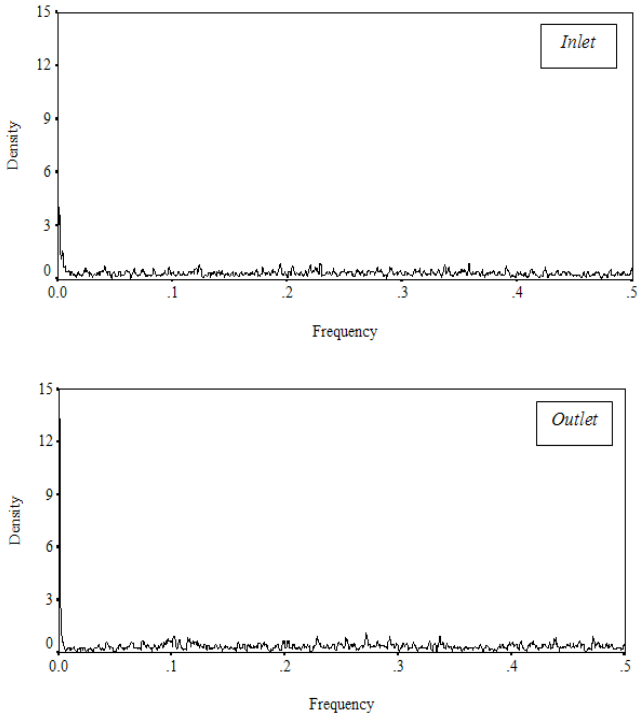

Figure 11: The Power Spectral Density for U_{LS} of 0.0155 and U_{LG} of 6.70 m/sec.

Figure **11** shows that despite the low range of energy fluctuation, it could be easily recognized that the density fluctuation is clearer at the outlet point than that appears at the inlet point. In other words, as long as the flow maintains its stratified pattern, no much

energy dissipation would take place during the flow across the bend.

5.2. Evaluation of the Stratified Flow Pressure Drop Model

The semi-empirical model discussed in this work has been used to compare experimental and predicted superficial water velocities. Figure **12** shows the results:

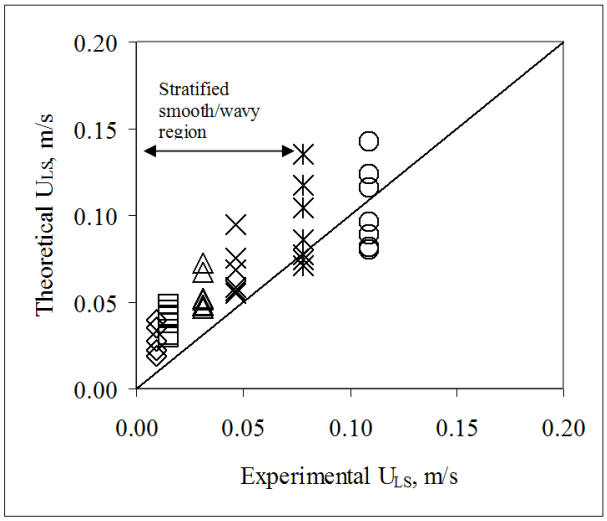

Figure 12: Experimental and theoretical superficial water velocities.

For the stratified flow, the comparison is acceptable as the superficial gas velocity increases. The overall comparison for stratified flow seems satisfactory since the values are not out by several orders of magnitude. The mismatch could be attributed to the gross assumption of having steady and developed flow in a bend.

As discussed earlier, while working on the force balance formulations to compute the pressure drops , it was found that there is a need to assign a value for $\frac{\partial h_L}{R\partial\theta}$ in order to obtain equality of pressure gradients for the air and water phases. If this is ignored, then the pressure gradients cannot be made to match, which violates the physics.

In a straight pipe, fully developed steady flow mean $\frac{\partial h_L}{\partial x}$ is zero. As anticipated, this is not exactly true for bend because the water level rises/falls across a bend for steady and fully developed flow.

Figure **13** shows a comparison between the experimental and theoretical pressure drop gradient for stratified air-water flow:

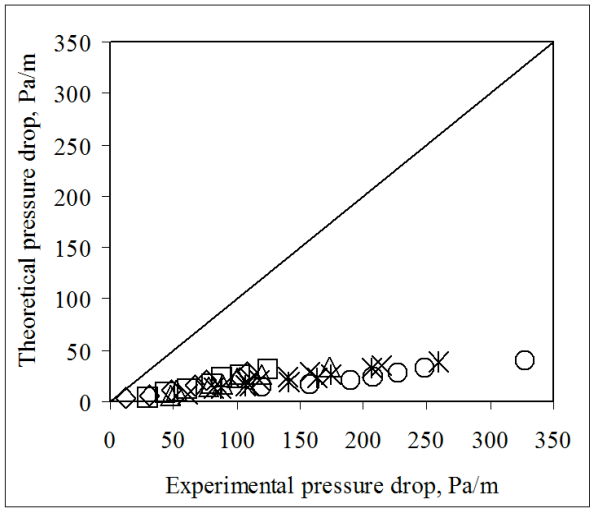

Figure 13: Experimental and theoretical pressure drop for stratified air-water flow.

The experimental values are much higher than the predicted due to compressibility effect. Compressibility of air cause a rise and drop in the upstream and downstream pressures, respectively. . Therefore, the experiments' results are with higher pressure drop than the theoretical value (as air assumed incompressible in the theory).

The liquid level gradient shows rising liquid height in most of the cases and this is consistent with the back pressure effect caused by the bend.

6. CONCLUSIONS

The following conclusions could be drawn from this study:

1. The pressure drop across the bend depends significantly on the flow pattern. This justifies the failure of the existing correlations to predict the pressure drop across the bend accurately.

2. It is more convenient to describe the pressure drop in terms of the energy loss. This is mainly due to the disturbance nature of the two-phase flow.

3. Using the power spectrum technique to describe the pressure drop was found to be more reliable.

4. The results acquired from the experiments have shown that the stratified flow does not cause a significant change in the energy during the flow along the bend traverse. The energy fluctuates higher with relatively higher air velocity due to the existence of the interfacial waves which create the disturbance.

5. The semi-empirical model developed for predicting the superficial water velocity during stratified flow shows an acceptable agreement with the experimental data. Even though the model was derived for the stratified flow, seems it yields acceptable results for slug flow as well in comparison with the experimental data.

6. The pressure drop values estimated by this model did not match well with the experimental data.

7. The time series acquired from the top part of the bend give a qualitative description to the flow across the bend.

NOMENCLATURE

A cross sectional area

g gravitational acceleration

h liquid level

P pressure

R radius of curvature of the bend

t time

U axial average velocity

Greek Letters

γ tilt angle of the symmetry line of the liquid lump from the gravitational direction

θ radial angle (location) of the fluid element

ρ phase density

τ shear stress

Subscripts

G gas

i interface

L liquid

S superficial

REFERENCES

[1] Singh MP. Entry flow in curved pipe. Journal of Fluid Mechanics 1974; 65: 517-539. http://dx.doi.org/10.1017/S0022112074001522

[2] Yao LS, Berger SA. Entry flow in a curved pipe. Journal of Fluid Mechanics 1975; 67: 177-196. http://dx.doi.org/10.1017/S0022112075000237

[3] Smith FT. Fluid flow into a curve pipe. Proceedings of the Royal Society of London. Series A: Mathematical and Physical Sciences 1976; A 351: 71-87.

[4] Stewartson K, Cebeci T, Chang KC. A boundary-layer collision in a curved duct. Quarterly Journal of Mechanics and Applied Mathematics 1980; 33: 59-75. http://dx.doi.org/10.1093/qjmam/33.1.59

[5] Berger SA, Talbot L, Yao LS. Flow in curved pipes. Annual Review of Fluid Mechanics 1983; 15: 461-512. http://dx.doi.org/10.1146/annurev.fl.15.010183.002333

[6] Soh WY, Berger SA. Laminar entrance flow in a curved tube. Journal of Fluid Mechanics 1984; 148: 100-135. http://dx.doi.org/10.1017/S0022112084002275

[7] Bovendeerd PHM, Van Steenhoven AA, Van De Vosse FN, Vossers G. Steady entry in a curved pipe. Journal of Fluid Mechanics 1987; 177: 233-246. http://dx.doi.org/10.1017/S0022112087000934

[8] Olson DE. Fluid mechanics relevant to respiration: flow within curved or elliptical tubes and bifurcating systems 1971; PhD Thesis, University of London, UK.

[9] Agrawal YY, Talbot L, Gong K. Laser anemometer study of flow development in curved circular pipe. Journal of Fluid Mechanics 1978; 85: 497-518. http://dx.doi.org/10.1017/S0022112078000762

[10] Choi US, Talbot L, Cornet I. Experimental study of wall shear stress in the entry region of a curved tube. Journal of Fluid Mechanics 1979; 93: 465-489. http://dx.doi.org/10.1017/S0022112079002603

[11] Olson DE, Snyder B. The upstream scale of flow development in curved circular pipes. Journal of Fluid Mechanics 1985; 150: 139-158. http://dx.doi.org/10.1017/S0022112085000064

[12] Edwards MF, Jadallah MSM, Smith R. Head losses in pipe fittings at low Reynolds numbers. Chemical Engineering Research and Design 1985; 63: 43-50.

[13] Fiedler HE. A note on secondary flow in bends and bend combinations. Experiments in Fluids 1997; 23: 262-264. http://dx.doi.org/10.1007/s003480050109

[14] Sudo K, Sumida M, Hibara H. Experimental investigation on turbulent flow in a circular-sectioned 90° bend. Experiments in Fluids 1998; 25: 42-49. http://dx.doi.org/10.1007/s003480050206

[15] Sudo K, Sumida M, Hibara H. Experimental investigation on turbulent flow in a circular-sectioned 180° bend. Experiments in Fluids 2000; 28: 51-57. http://dx.doi.org/10.1007/s003480050007

[16] Hwang NHC, Hita CE. Fundamentals of Hydraulic Engineering Systems, 2nd edition 1987; New York, USA, Prentice-Hall.

[17] Idel'chik IE. Flow resistance. A Design Guide for Engineers. New York, Hemisphere Publishing Corporation 1989.

[18] Ito H. Flow in curved pipes. International Journal of the Japanese Society of Mechanical Engineers 1987; 30: 262.

[19] Roberson HA, Crowe CT. Engineering Fluid Mechanics, 6th edition 1997; USA, John Wiley & Sons.

[20] Munson BR, Young DF, Okiishi TH. Fundamentals of Fluid Mechanics, 3rd edition 1998; USA, John Wiley & Sons.

[21] Azzi A, Friedel L, Belaadi S. Two-phase gas/liquid flow pressre loss in bends. Forschung im Ingenieurwesen 2000; 65: 309-318. http://dx.doi.org/10.1007/s100100000030

[22] Robertson JG. Pressure loss coefficient for 90o circular bends. HTFS 1979; RS 270.

[23] Hooper WB. The two-K method predicts head losses in pipe fittings. Chemical Engineering 1981; 88: 96-100.

[24] Gardner GC, Neller PH. Phase distributions in flow of an air-water mixture round bends and past obstructions at the wall of a 76-mm bore tube. Proc Instn Mech Engrs-Part 3C 1969; 184: 94-101.

[25] Maddock C, Lacey PMC, Patrick MA. The structure of two-phase flow in a curved pipe. Institution of Chemical Engineers Symposium Series 1974; No. 38.

[26] Azzopardi BJ, Sudlow CA. The effect of pipe fittings on the structure of two-phase flow. Proceeding of the UIT Conference, Milano Italy 1993.

[27] Khaksafard R, Tajalipour N, Paraschivoiu M, Teevens PJ, Zhu Z. CFD Based Analysis of Multiphase Flows in Bends of Large Diameter Pipelines. NACE International Corrosion Conference & Expo 2013; Paper No. 2480.

[28] Xing L, Yeung H. Investigation of slug flow induced forces on pipe bends applying STAR-OLGA coupling 2011; BHR Group 2011 Multiphase 15.

[29] Belfroid SPC, Schiferli W, Cargnelutti MF, M van Osch. Forces on bends and T-joints due to multiphase flow 2010; BHR Group 2010 Multiphase 7.

[30] Alwazzan A. Two-Phase Flow Through Horizontal Pipe With Elbow. PhD Thesis University of Malaya 2006.

[31] Chisholm D. A theoretical basis for the Lockhart-Martinelli correlation for two-phase flow. International Journal of Heat and Mass Transfer 1967; 10: 1767-1778. http://dx.doi.org/10.1016/0017-9310(67)90047-6

[32] Chisholm D. Pressure losses in bends and tees during steam-water flow. NEL Report No. 318 1967.

[33] Kuhn HG, Morris SD. presented by Azzi *et al*., 2000 as private communication 1997.

[34] Sookprasong P. Two-phase flow in piping components. MSc thesis, University of Tulsa, Tulsa, Oklahoma, USA 1980.

[35] Paliwoda A. Generalized method of pressure drop calculation across pipe component containing two-phase flow of refrigerant. Revue Internationale du Froid 1992; 15(2): 120-126. http://dx.doi.org/10.1016/0140-7007(92)90036-T

Received on 13-02-2015 Accepted on 25-02-2015 Published on 20-04-2015

DOI: http://dx.doi.org/10.15377/2409-787X.2015.02.01.4